AFTERSHOCKS AND PREEARTHQUAKE SEISMICITY[1]

By CARL E. JOHNSON,
U.S. GEOLOGICAL SURVEY;

and

L. K. HUTTON,
CALIFORNIA INSTITUTE OF TECHNOLOGY

CONTENTS

ABSTRACT

Although primary surface faulting was mapped for nearly 30 km, aftershocks extended in a complex pattern more than 100 km along the trend of the Imperial fault. A first-motion focal mechanism for the main shock is consistent with right-lateral motion on a vertical fault striking N. 42° W., in agreement with the strike of the Imperial fault within the limits of resolution. There is evidence that conjugate faulting on a buried complementary northeast-trending structure occurred at the north limit of displacement on the Imperial fault near Brawley, Calif. This faulting was apparently initiated at the time of a magnitude 5.8 aftershock 8 hours after the main shock. A line of epicenters extending along the trend of the San Andreas fault nearly 100 km into the eastern Imperial Valley was noted during the aftershock sequence, in an area recognized as notably aseismic during the preceding 5 years. The main shock was preceded by a 3-month period of significantly reduced seismicity affecting the central Imperial Valley. Although three small events near the incipient epicenter during this interval may be deemed foreshocks, no distinct foreshocks immediately before the main shock were observed.

INTRODUCTION

The Imperial Valley earthquake of October 15, 1979, was the largest in California since the installation of dense seismic networks and thus provides a unique opportunity for studying both the aftershocks and prior seismicity of a moderate earthquake in a detail never before possible. During the next few years we expect that the tens of thousands of digital seismograms for several thousand aftershocks, together with a large body of other geophysical data, will provide the basis for many inquiries into the physical processes attending major earthquakes. Here we provide only a preliminary and incomplete picture of the most conspicuous of these phenomena.

Our ideas are not presented chronologically. We first discuss gross aspects of the aftershock distribution and then place it within a context of seismicity during the preceding years. Having discussed what appears to have been normal background seismicity for the central Imperial Valley, we can then consider possibly unusual aspects of activity during the weeks immediately before the main shock.

ANALYSIS

Our data are from 150 short-period vertical instruments in the southern California seismic network operated jointly by the California Institute of Technology (CIT) and the U.S. Geological Survey (USGS). These data were telemetered in analog form to CIT, where they were digitized at 50 Hz. A real-time event detector recorded selected intervals of record on magnetic tape for subsequent offline analysis on an interactive cathode-ray-tube (CRT) display terminal.

Both the event locations and magnitudes reported here (table 7) are preliminary results from the first stage of routine processing, using the CEDAR system described by Johnson (1979). Final values will not be available until much more editing and analysis of the data have been completed. Processing of the more than 2,000 aftershocks that occurred during the first 20 days after the earthquake required the accurate timing of more than 40,000 discrete arrivals. Hypocenters were calculated using an unpublished program (QED1) de-

[1]Contribution No. 3459, Division of Geological and Planetary Sciences, California Institute of Technology, Pasadena, CA 91125.

TABLE 7.—*Preliminary origin times, epicentral coordinates, and local magnitudes for aftershocks of* $M_l \geq 4.0$

Date	Origin time (G.m.t.)	Epicentral coordinates		Local magnitude (M_l)
		Latitude N.	Longitude W.	
10/15	2316:53.44	32°36.82′	115°19.09′	6.6
	2319:29.98	32°45.94′	115°26.45′	5.0
	2325	----	----	4.0
	2355:03	32°55′	115°31′	[1]4.2
10/16	0022:14.20	32 57.46′	115°31.19′	4.2
	0100:13.86	32°57′	115°29′	[1]4.6
	0114:21.29	32°55.54′	115°31.38′	4.3
	0139:04	32°56.45′	115°31.45′	4.0
	0310	----	----	4.5
	0316:25.43	32°56.73′	115°32.56′	4.1
	0339	----	----	4.5
	0549:10.18	32°56.63′	115°32.38′	5.0
	0604:39.03	32°54.79′	115°32.07′	4.1
	0611:59.96	32°56.05′	115°30.88′	4.2
	0613:13.41	32°55.45′	115°31.60′	4.2
	0619:48.68	32°55.71′	115°32.36′	5.1
	0655	----	----	4.6
	0658:42.69	32°59.83′	115°34.41′	5.8
	0723:24.21	32°53.92′	115°31.12′	4.2
	0749	----	----	4.0
	0936:41.14	32°56.31′	115°30.87′	4.0
	1051:27.11	32°56.34′	115°33.02′	4.0
	1126:27.40	32°57.83′	115°35.19′	4.0
	1146	----	----	4.8
	1201:44.96	32°52.31′	115°31.07′	4.0
	1500	----	----	4.0
	2316	----	----	4.9
10/17	1914:37.72	32°54.39′	115°35.00′	4.2
	2052	----	----	4.2
	2245	----	----	4.6
10/19	1222	----	----	4.1

[1]Epicentral location in error by 5 km or more.

veloped at CIT, based on the generalized inverse method formalized by Wiggins (1972). The crustal model used for all hypocentral calculations (table 8) was obtained graphically from the models presented by Mooney and McMechan (this volume), using data obtained during the Imperial Valley seismic-refraction experiment discussed by Fuis and others (this volume). This model is representative of the central Imperial Valley south of Brawley, Calif. Most magnitudes greater than 3.0 are standard M_L's from peak amplitudes on Wood-Anderson torsion seismometers; the remaining magnitudes are M_{ca}'s calculated from coda amplitudes, using the method of Johnson (1979). Focal mechanisms were obtained using the computer program described by Whitcomb (1973).

TABLE 8.—*Crustal model used for locating aftershocks*

Depth to top of layer (km)	Layer velocity (km/s)
0	2.15
1	2.75
2	3.60
3	4.30
4	5.05
5	5.50
5.5	5.70
10.0	5.80
13.0	6.95
14.0	7.20
25.0	7.80

We selected events for analysis and graphic presentation solely on the basis of location quality (epicentral error, less than 5 km), a criterion that generally favors the largest events during a given period. Some events of magnitude larger than 4.0 have been ignored either because they were immediately preceded by others large enough to make accurate timing difficult or because they occurred during an interval for which digital data were not available.

AFTERSHOCK DISTRIBUTION

Figure 32 illustrates all well-located aftershocks that occurred during the first 20 days of the aftershock sequence (October 15 through November 5). The main shock, denoted by the star south of the United States-Mexican border, lies within a zone that remained surprisingly aseismic throughout the sequence. A more accurate epicenter for the main shock, obtained by Chavez and others (this volume) using a balanced suite of U.S. and Mexican data, plots about 2 km to the northeast, midway between the location shown on the map (fig. 32) and the United States-Mexican border.

The focal mechanism for the main shock (lower right, fig. 32) is consistent with right-lateral motion on a vertical fault striking N. 42° W., in general agreement with the trend of the southern section of the Imperial fault. Although surface breaks were limited to a zone 30 km long (heavy lines, fig. 33), aftershocks occurred within an area 110 km long, from the Cerro Prieto geothermal area to the Salton Sea. Except for one small group of events near the south terminus of surface rupture, most aftershocks were clustered within about 15 km of Brawley, particularly during the first 8 hours after the main shock (fig. 33).

A significant change in the aftershock distribution occurred after the largest aftershock (M_L=5.8) at 0658 G.m.t. October 16, approximately 8 hours after the main shock and immediately after the interval plotted in figure 33. The location of this event, here referred to as the Brawley aftershock, is marked by its focal mechanism, plotted west of Brawley on the map (center, fig. 32). The most distinctive change in the aftershock pattern was a strong northeast-trending line of epicenters from west of Brawley to just south of Wiest Lake (WLK, figs. 32, 33), in agreement with the left-lateral plane of the focal mechanism. Tectonically the local increase in strain at the north end of the Imperial fault break was apparently accommodated by left-lateral motion on a conjugate fault propagating from southwest to northeast. Independent support for this conclusion is provided by a coincident linear zone of ground disturbance, liquefaction, and cracking mapped by T. H. Heaton, J. G. Anderson, and P. T. German (unpub. data, 1980). Unfortunately, fieldwork was complicated by slumping

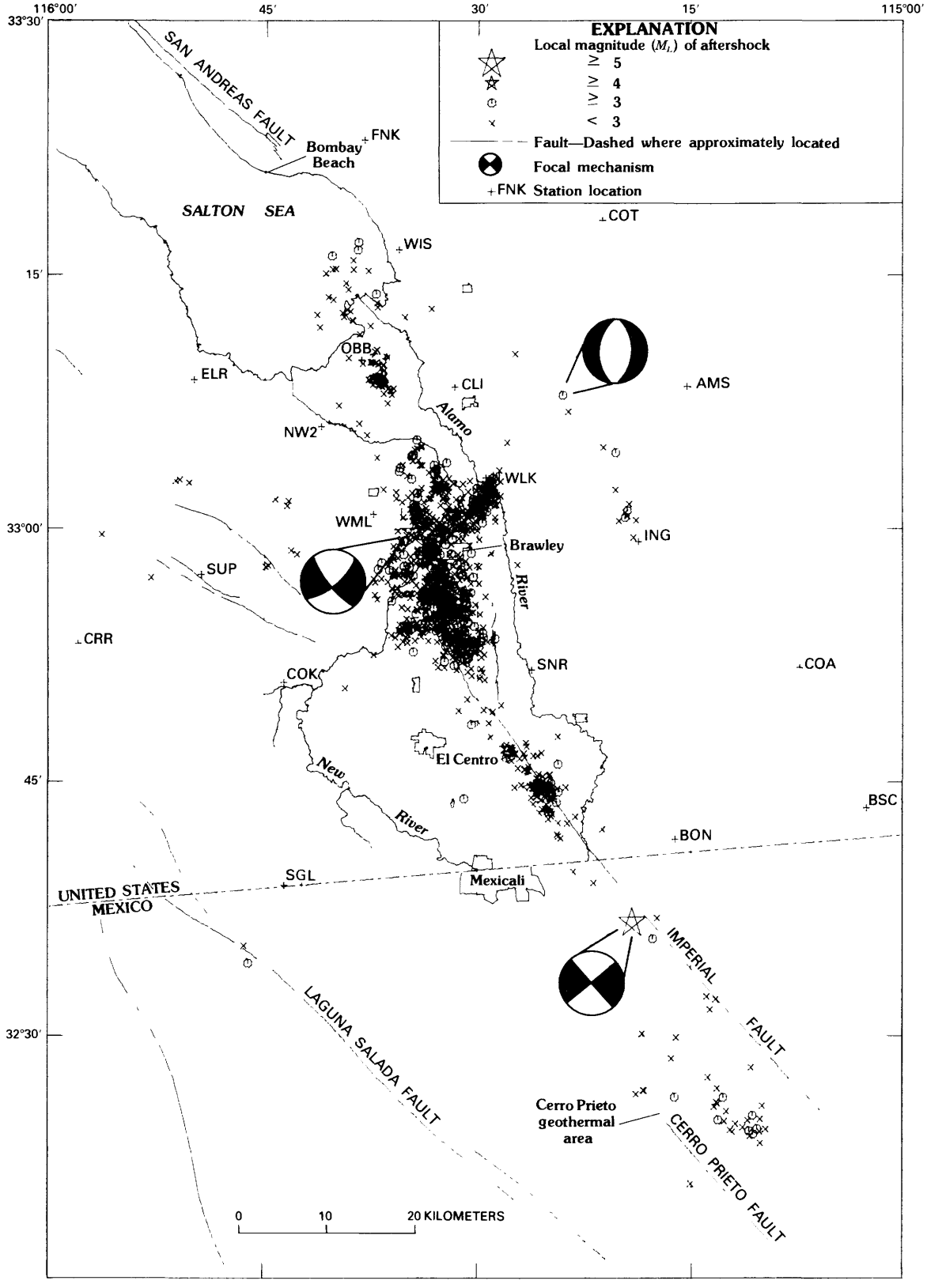

FIGURE 32.—Well-located aftershocks (epicentral error, less than 5 km) from October 15 through November 5, 1979. Focal mechanisms are lower-hemisphere equal-area projections with compressional quadrants darkened. Star denotes location of main shock.

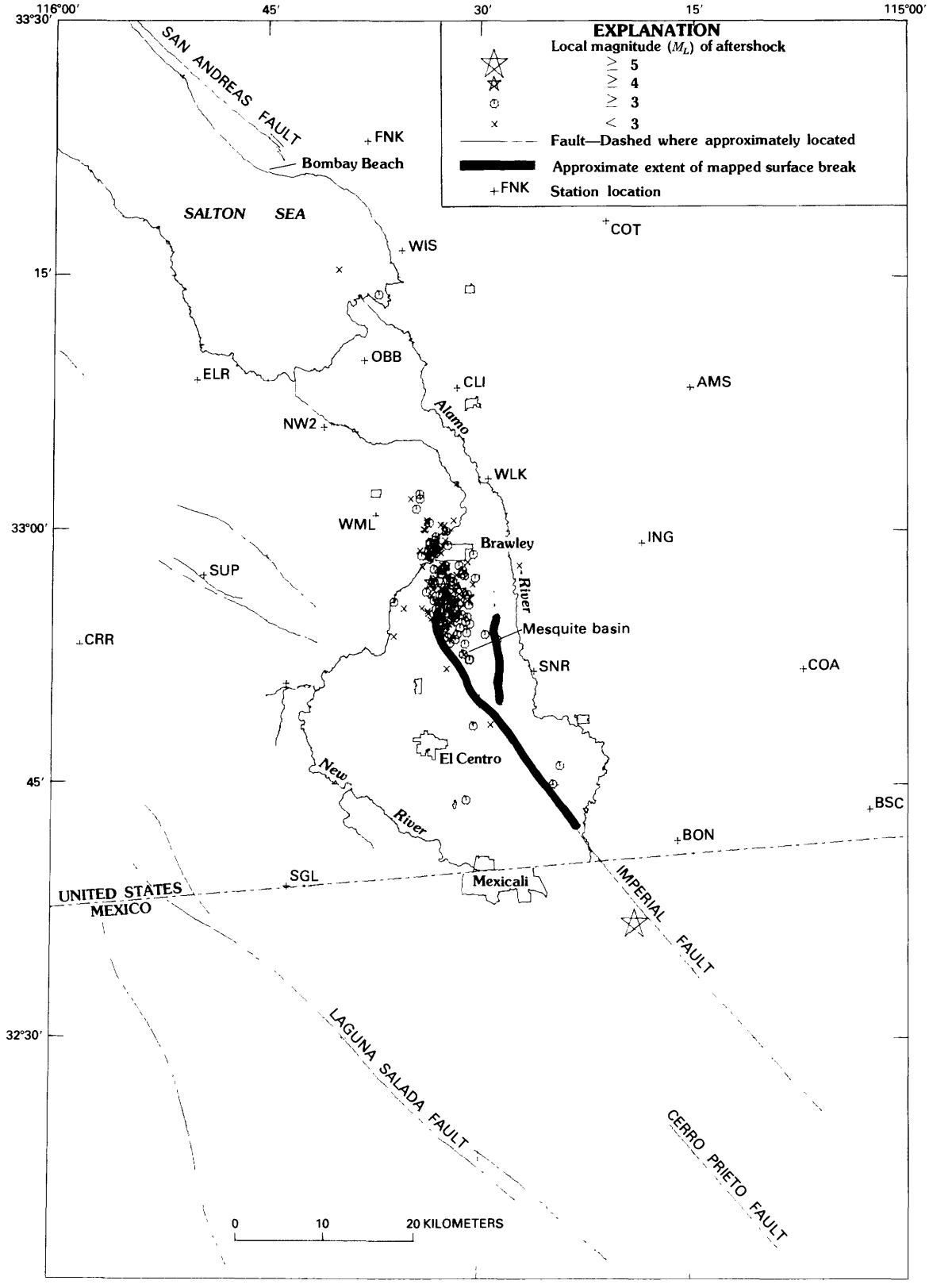

FIGURE 33.—Well-located aftershocks during first 8 hours of aftershock sequence.

of the south bank of the New River along much of the suggested structure.

Historically, conjugate faulting near Brawley does not appear to be unusual. A similar explanation was offered by Johnson and Hadley (1976) for arcuate northeast-trending breaks that were mapped along the northwest margin of the Mesquite basin after the 1940 earthquake. Their explanation was based primarily on lineations in seismicity and focal mechanisms from an earthquake swarm near Brawley during January 1975. The 1940 earthquake was also followed within several hours by an aftershock (M_L=5.5) that was more destructive at Brawley than was the 1940 main shock. This aftershock has generally been associated with delayed rupture on the Imperial fault unilaterally northward from the instrumental epicenter (see Trifunac and Brune, 1970; Johnson, 1979), following Richter (1958). However, in light of observations from the 1979 event, it appears that this earthquake may have occurred on a conjugate structure similar, if not identical, to that of the 1979 Brawley aftershock.

One of the most intriguing features apparent on the aftershock-distribution map (fig. 32) is a line of events that extends along the trend of the San Andreas fault 50 km into the Imperial Valley. As discussed by Johnson (1979), this part of the valley was virtually aseismic through 1978, since the installation of a dense seismograph network in mid-1973. The first events along this trend occurred in 1979 (discussed below) before the main shock. Although few of these events were large enough to provide well-constrained focal mechanisms, nevertheless, first motions are generally consistent with the normal focal mechanism shown in figure 32 for one of the largest events. An abrupt increase in activity along this trend after the main shock leaves little doubt that these events represent a response to the changes in stress associated with the main shock and thus can be considered aftershocks. Mechanically they may represent valley subsidence along an ancient strand of the San Andreas fault, particularly because they all occurred within the dilatational quadrant of the static-strain field associated with the main shock.

The development of the aftershock distribution over time is most clearly revealed by a series of time-distance plots (figs. 34–36) projected onto the Imperial fault. Events were selected from the solid parallelepiped shown in figure 37, with distances measured from its southeast corner. These three plots, covering 1, 3, and 23 days after the main shock, respectively, provide a reasonably complete picture of the temporal development of the aftershock pattern. A virtually aseismic zone separates the region of clusters of aftershocks during the first 12 hours (fig. 34) from the area of the main shock. After 12 hours an increase in activity outside the initial cluster seems to mark the beginning of a general expansion of the aftershock region both to the north and to the south (fig. 35). This expansion, which appears to be progressive over time, culminated in the north with a cluster of events near the south end of the Salton Sea, and in the south with a cluster centered near the Cerro Prieto geothermal area. Once it began, activity at each of several clusters along the Imperial fault tended to persist. If we associate a migration rate with the onset of activity at each cluster, based on a point of initiation near Brawley at the time of the main shock, a velocity of just less than 2 km would be appropriate. This rate is faster than the value of 0.2 to 1.0 km/d reported by Johnson (1979) for the characteristic velocity relating clusters with sequences of earthquake swarms along the same trend, but is much slower than the 12-km/d rate reported by Johnson and Hadley (1976) for the bilateral development of a large earthquake swarm on the Brawley fault zone (eastern branch of surface break, fig. 33) in January 1975. Migration at widely varying rates appears to be a general feature of earthquake sequences within the Imperial Valley.

HISTORICAL PERSPECTIVE

The phenomena accompanying recent faulting in the Imperial Valley can best be understood within a context of the historical seismicity of this region. In this section we touch briefly on the most important aspects of a more detailed discussion by Johnson (1979). Figures 37 and 38 provide an overview of the seismicity in the Imperial Valley during the 6 years since the installation of a dense seismic network in 1973. The most obvious feature on the seismicity map (fig. 37) is a pod-shaped area of seismicity connecting the Imperial fault north of Mexicali, Mexico, with the San Andreas fault near Bombay Beach. This area, termed the "Brawley seismic zone" by Johnson (1979), probably marks a zone of concentrated deformation associated with the transfer of displacement from the Imperial fault to the south end of the San Andreas fault. Its shape is identical to that of the pod-shaped intrusive zones in Hill's (1977) model for Imperial Valley tectonics as a manifestation of a leaky transform fault, although the zone is somewhat larger than he suggests. Another similar zone of seismicity connects the Imperial and Cerro Prieto faults at the lower part of figure 37. The sparseness of high-quality epicenters here is due to inadequate location capability rather than intrinsically lower activity. We note that the tectonic similarity between these two areas is strongly reflected in the seismicity patterns.

Both the 1940 and 1979 earthquakes originated near an apex of one of these two seismic zones (fig. 37). Because the site of maximum faulting was south of the instrumental epicenter, Richter (1958) and Trifunac

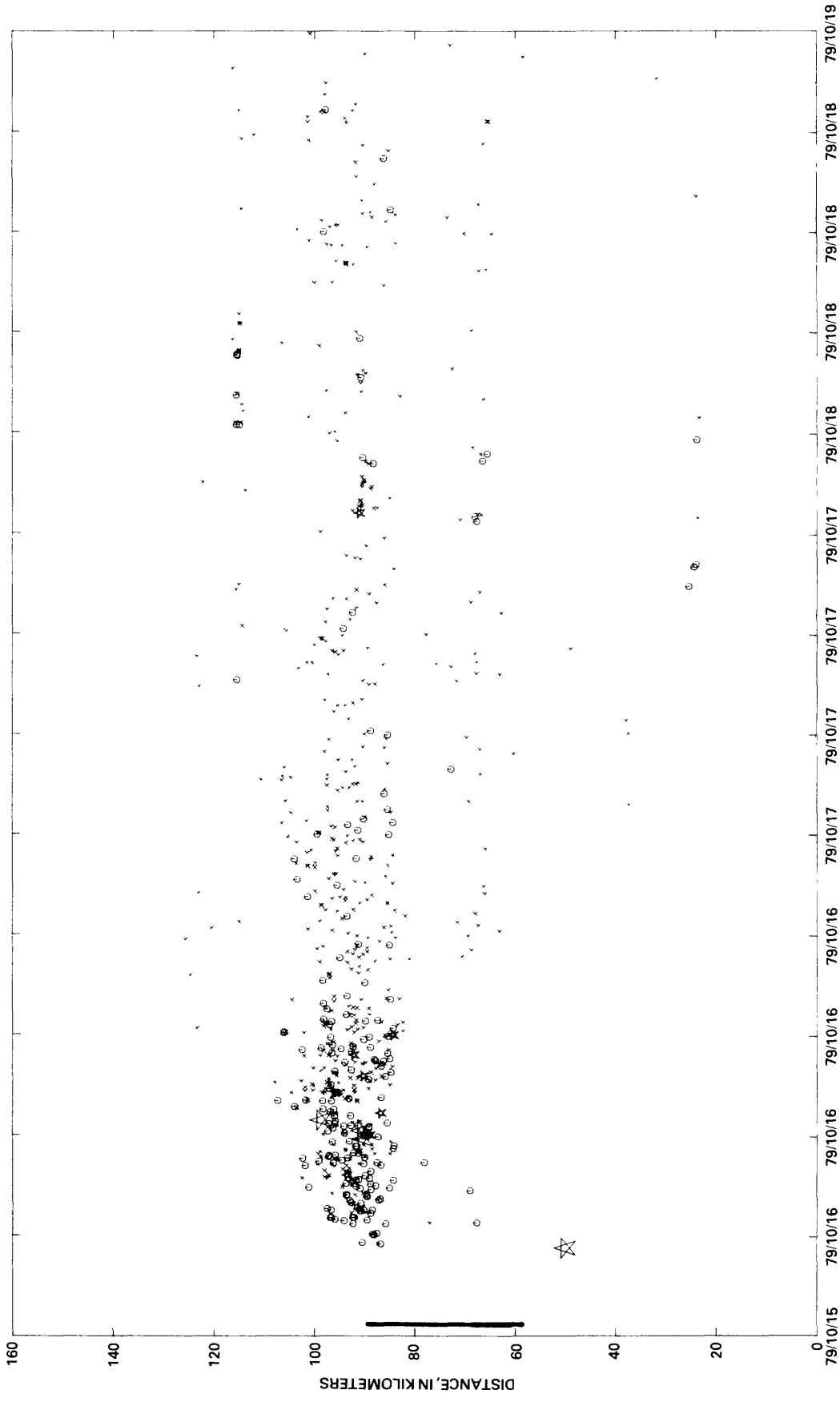

FIGURE 34.—Time as a function of distance for first 24 hours of aftershocks, projected onto trend of Imperial fault. Distance is measured from lat 32°15′ N., long 115°00′ W. (southeast corner, fig. 37). Line along distance axis of each graph shows extent of mapped surface breaks. Symbols for local magnitude same as in figure 32.

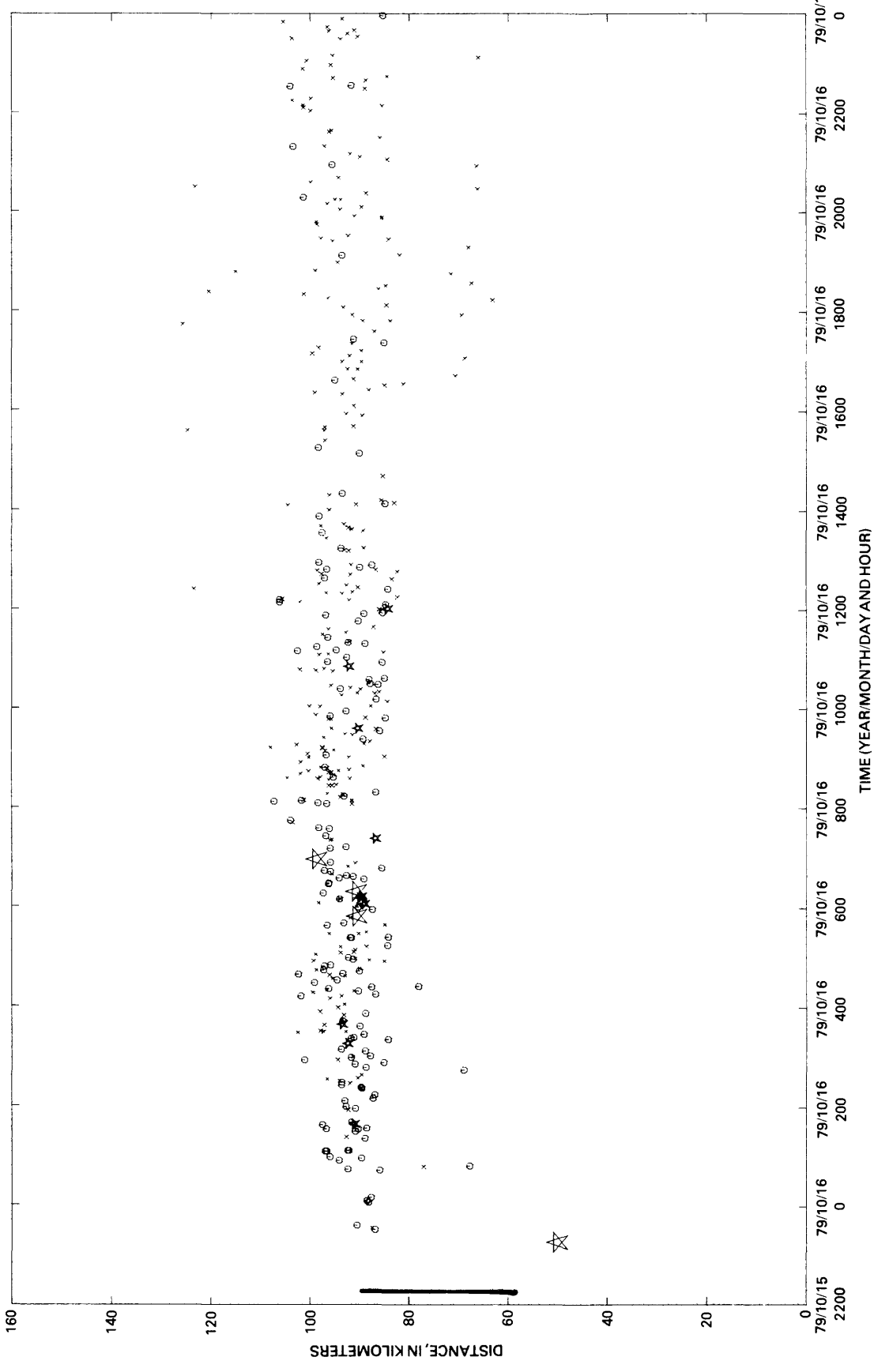

FIGURE 35.—Time as a function of distance for first 3 days of aftershocks, projected onto trend of Imperial fault. Distance is measured from lat 32°15′ N., long 115°00′ W. (southeast corner, fig. 37). Line along distance axis shows extent of mapped surface breaks. Symbols for local magnitude same as in figure 32.

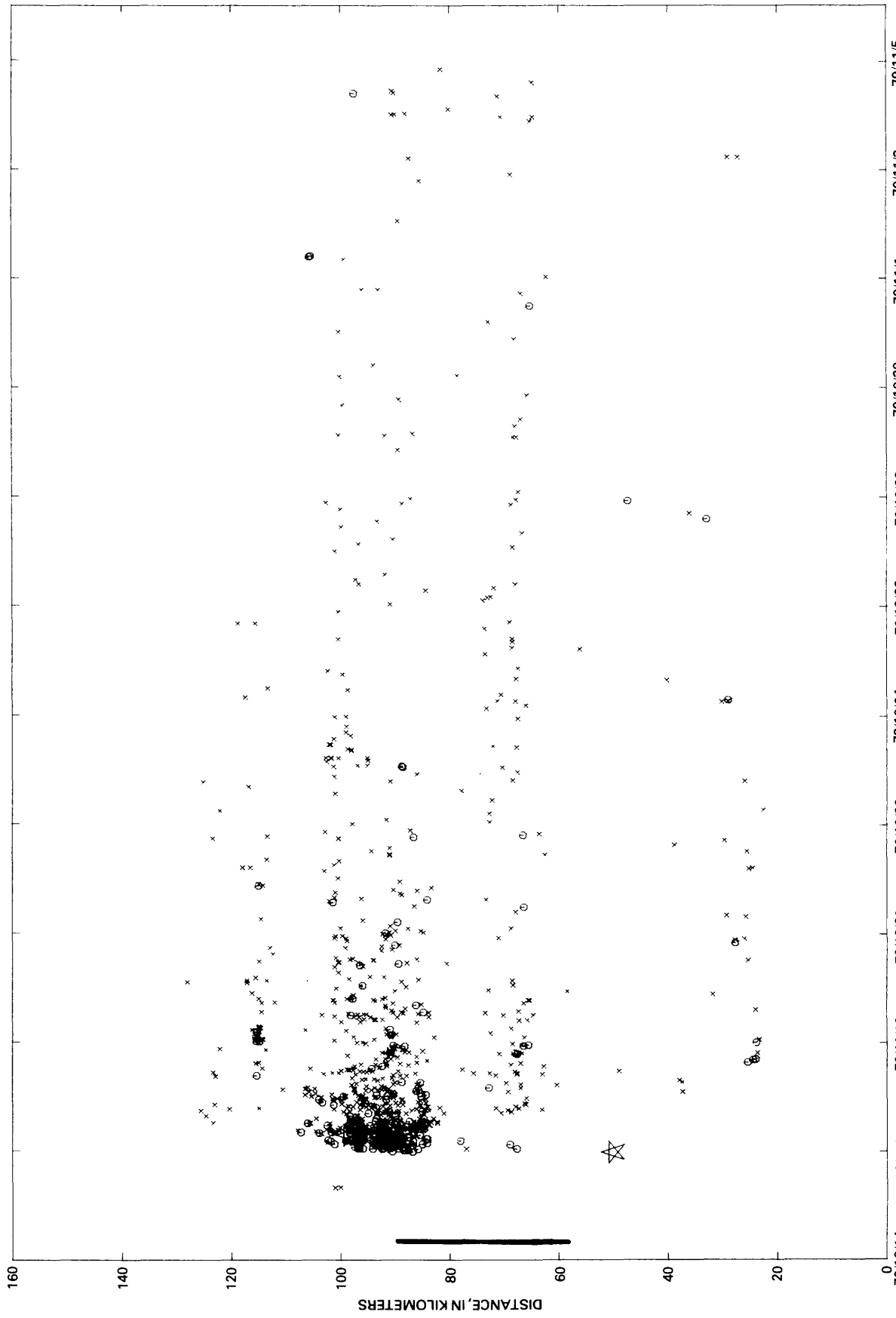

FIGURE 36.—Time as a function of distance for first 23 days of aftershocks, projected onto trend of Imperial fault. Distance is measured from lat 32°15′ N., long 115°00′ W. (southeast corner, fig. 37). Line along distance axis shows extent of mapped surface breaks. Symbols for local magnitude same as in figure 32.

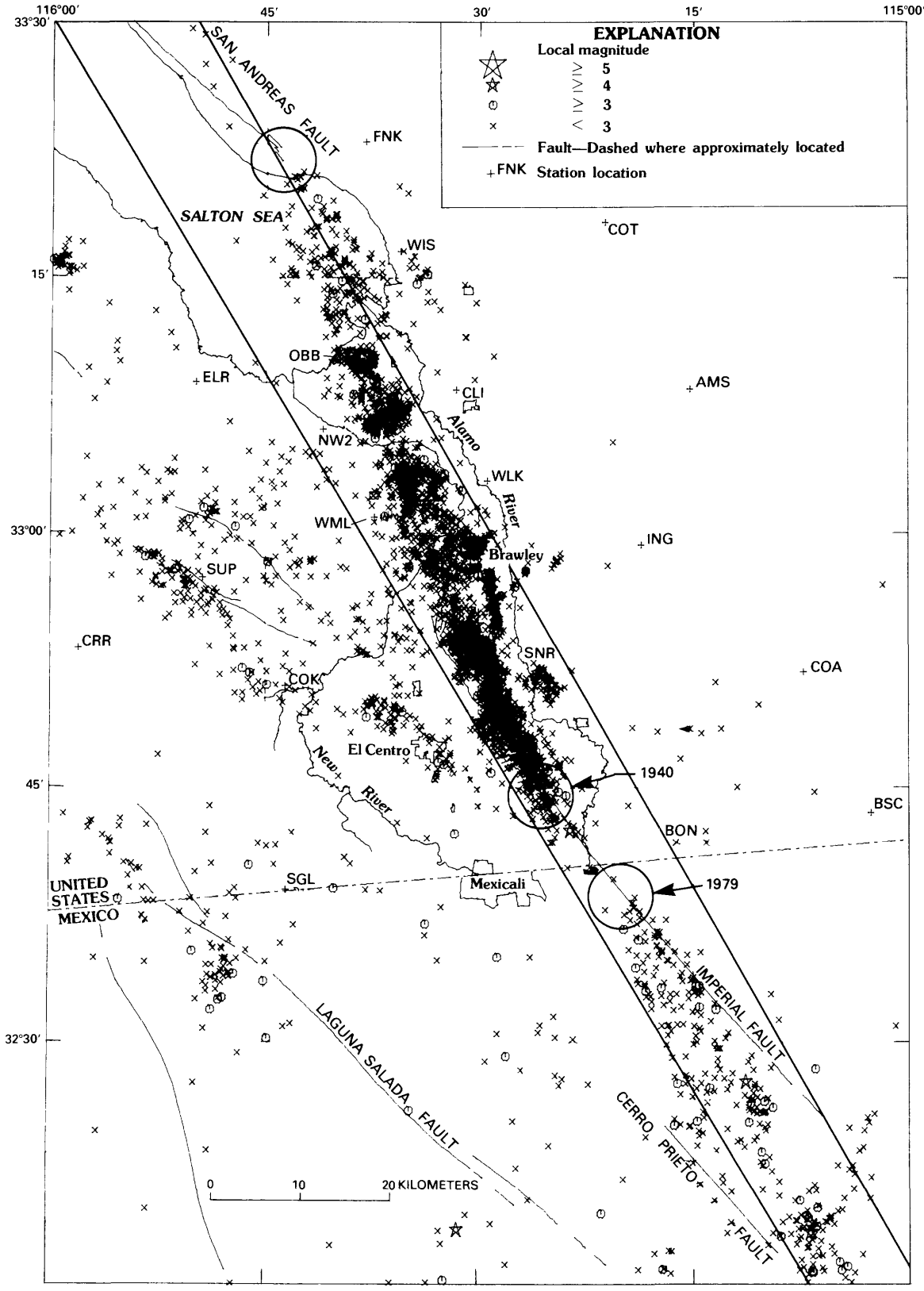

FIGURE 37.—Well-located earthquakes (epicentral error, less than 5 km) from installation of Imperial Valley seismic network in mid-1973 through September 1979. Southernmost circles denote epicentral regions of 1940 and 1979 Imperial Valley earthquakes; circle at north terminus of Brawley seismic zone indicates likely epicenter for major earthquakes on southern section of San Andreas fault. Area outlined in heavy lines defines section area for events shown in figures 34 through 36, 38, and 40.

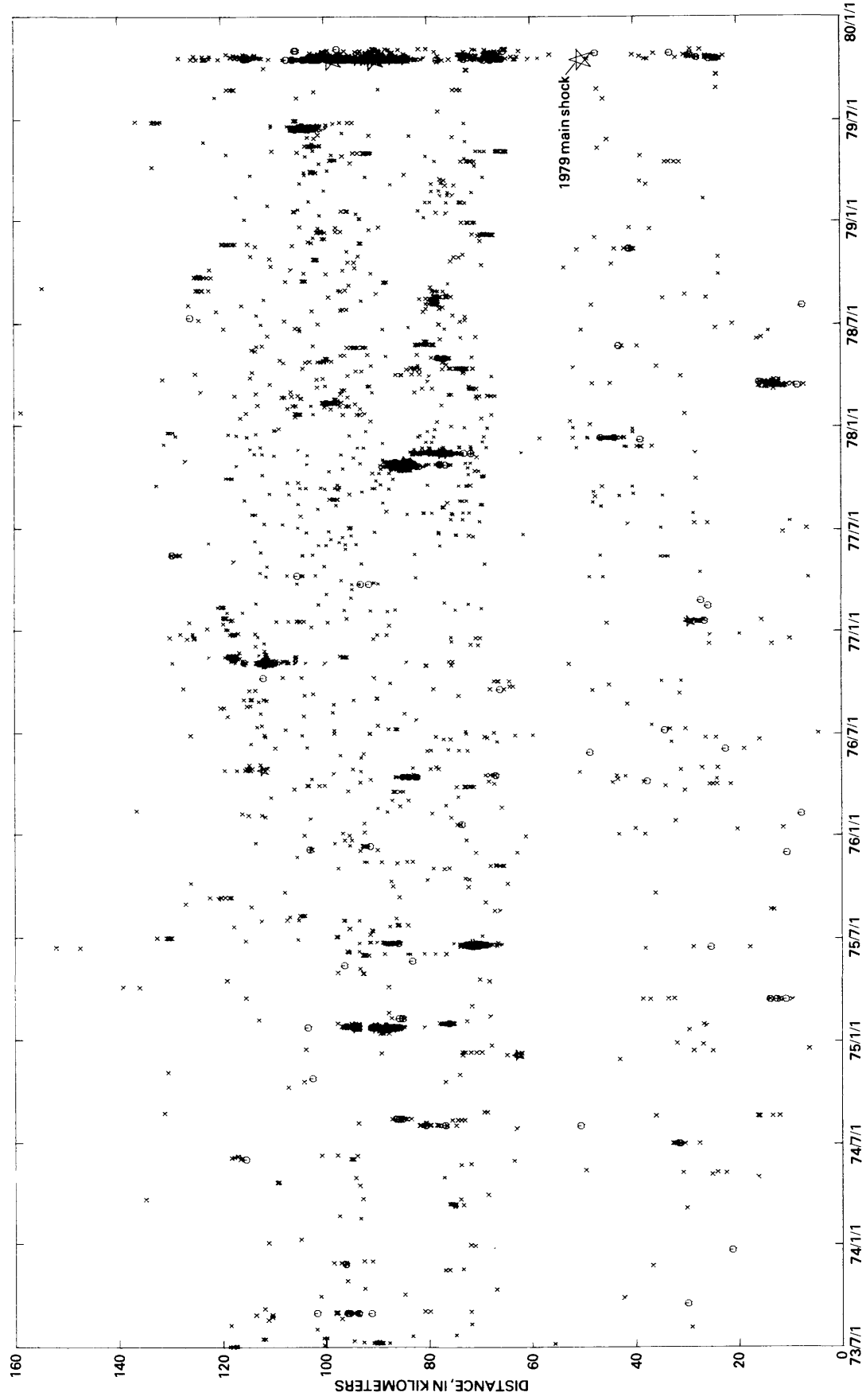

FIGURE 38.—Time as a function of distance for all well-located earthquakes along Imperial fault from mid-1973 through November 5, 1979. Distance is measured from lat 32°15′ N., long 115°00′ W. (southeast corner, fig. 37). Star denotes location of October 15 main shock. Symbols for local magnitude same as figure 37.

and Brune (1979) concluded that in 1940, rupture propagated southeastward across the aseismic zone straddling the United States-Mexican border. Similarly, the 1979 event apparently broke across the aseismic zone and this time propagated northward. If the two seismic zones represent regions of concentrated deformation, then their ends should represent points of concentrated loading on the major strike-slip faults. Strain energy stored in the "locked" aseismic section can be released periodically in moderate shocks. This concept is consistent with the observation by Johnson (1979) that episodic creep is confined to the seismic sections of the Imperial fault north of the border. There is no evidence for episodic creep within the aseismic sections, although continuously recording creepmeters have been in operation for several years at the Tuttle Ranch on the west bank of the Alamo River (Goulty and others, 1978). Nonepisodic creep rates of less than 2 mm/yr measured on an alinement array crossing the Imperial fault near the United States-Mexican border (reported by Goulty and others, 1978) are comparable to measurements for locked sections of the San Andreas fault near Indio, Calif., about 27 km northwest of the Salton Sea (Keller and others, 1978).

A similar tectonic relation exists at the north terminus of the Brawley seismic zone where it joins the San Andreas fault near Bombay Beach. This point (top circle, fig. 37) should be considered a likely epicenter for major earthquakes on the southern section of the San Andreas fault, in which rupture propagation would be to the northwest. More extensive tectonic instrumentation near this point seems prudent.

The correspondence between background seismicity and the intensity of aftershock activity along the Imperial fault can best be portrayed by a time-distance plot (fig. 38) covering the 6 years since the installation of the dense Imperial Valley network. Essentially, the spatial distribution of aftershocks mimics that of the preceding background: most events occur along previously seismogenic sections of the Imperial fault and avoid that section that was previously aseismic. The position of the main-shock epicenter at the south end of a persistent seismic gap and the predominance of aftershocks to the north are particularly clear on the plot. We note that this gap is not filled by the aftershock distribution.

The only event comparable to the 1979 main shock during the instrumental history of the Imperial Valley is the 1940 earthquake near El Centro. To facilitate a direct comparison, we reproduce here the Wood-Anderson seismograms recorded at Pasadena, Calif., for these two events (fig. 39). The main shock in 1979 appears relatively simple, and moderate aftershocks lasted throughout the first day; the initial shock in 1940 is considerably more complex, and all major aftershocks occurred within the first 1½ hours. This complexity was studied by Trifunac and Brune (1970), who concluded that substantial seismic energy was released at several discrete points along the Imperial fault as rupturing progressed southward. This conclusion implies that the energy release during the 1979 shock may have been more localized near the instrumental epicenter. The difference between the 1940 and 1979 events is also reflected in the difference in seismic moment: the 1940 event was about 10 times larger than the 1979 shock, although the local magnitude was somewhat smaller. Further analysis of the wealth of strong-motion data recorded during the 1979 main shock should greatly elucidate this comparison.

PREEARTHQUAKE SEISMICITY

One of the most important contributions from dense-seismic-network studies of moderate earthquakes is the determination of the presence or absence of phenomena that can be broadly classed as precursory. Possibly the most useful contribution to our study was evidence for a remarkable 40-percent decrease in seismicity during the 15 weeks immediately preceding the main shock. This decrease, apparently affecting seismicity all along the axis of the Imperial Valley, can be seen as a vertical swath of lower activity on the time-distance plot (fig. 38) and on the aftershock frequency distribution (fig. 40). Because the number of detected events is an objective measure of seismicity during the period in figure 40, the observed change is probably real. A change in the detection parameters toward the end of 1977 prevents a comparison with seismicity levels using the detectability criterion before this period.

The importance of this apparent seismicity change mandates considerable skepticism regarding its existence. A survey of the operational state of the stations in the Imperial Valley network did not reveal any problem that might increase the detection threshold sufficiently to account for the observed change. One possible problem concerns the implementaion of antialiasing filters affecting half of the Imperial Valley network on July 17, 1979. It was not anticipated that this change would reduce detectability—quite the contrary was intended. Similar changes throughout the rest of the southern California seismic network were not followed by a reduction in detection capability. In addition, the period of depressed seismicity appears to have commenced more than 2 weeks before the instrumentation change. To determine whether the remainder of this anomalous period could be related to properties of the instrumentation, a comparison was made with that part of routine processing dealing solely with the analysis of helicorder records for a subset of the network not affected by the

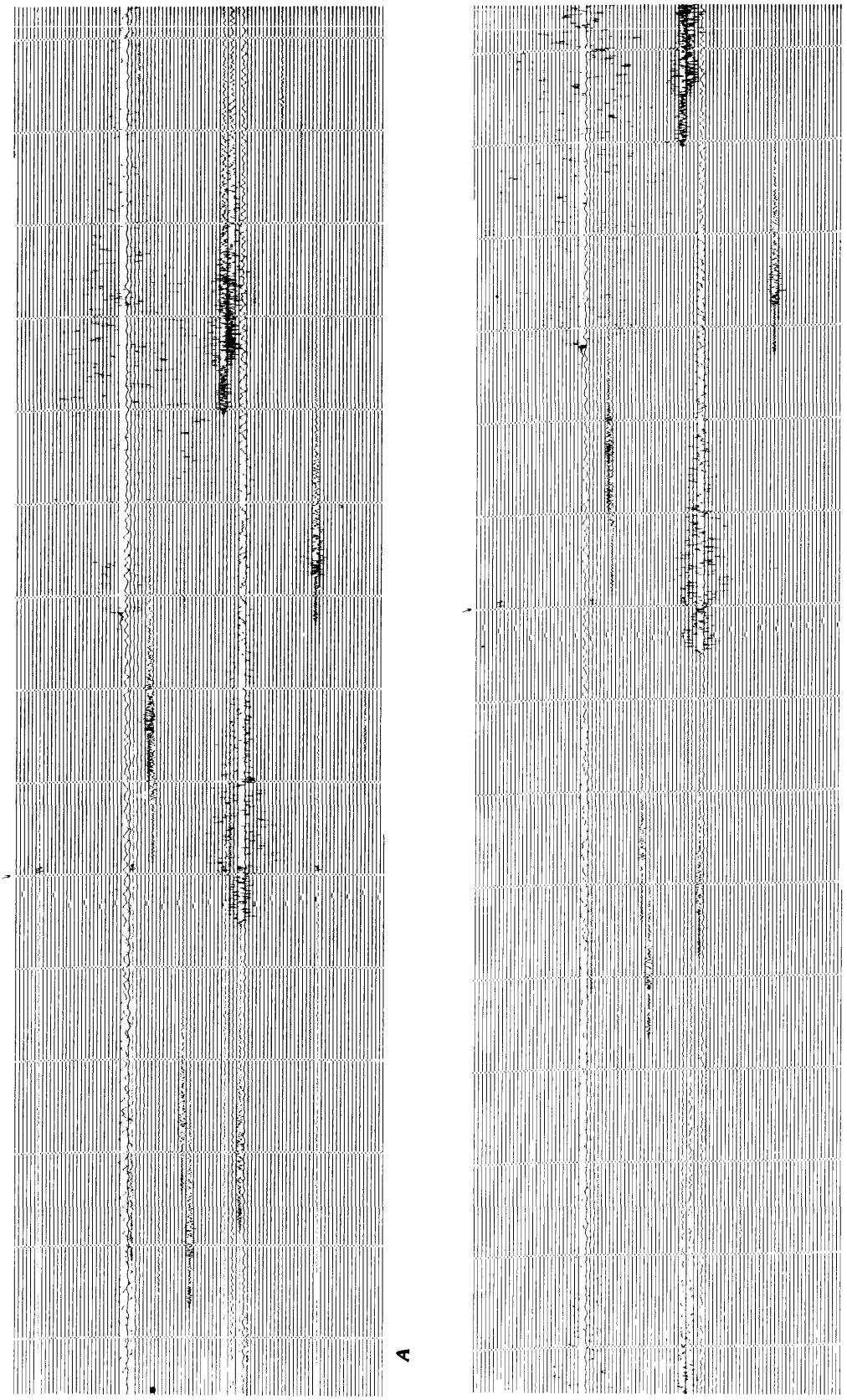

FIGURE 39.—Seismograms from Pasadena Wood-Anderson torsion seismometer. Marks and numbers on seismograms are made in routine record analysis. *A*, North-south component for 24-hour period beginning 1723 G.m.t. October 15, 1979. *B*, East-west component for 24-hour period beginning 1720 G.m.t. October 15, 1979. *C*, North-south component for 24-hour period beginning 1705 G.m.t. May 18, 1940. *D*, East-west component for 24-hour period beginning 1705 G.m.t. May 18, 1940.

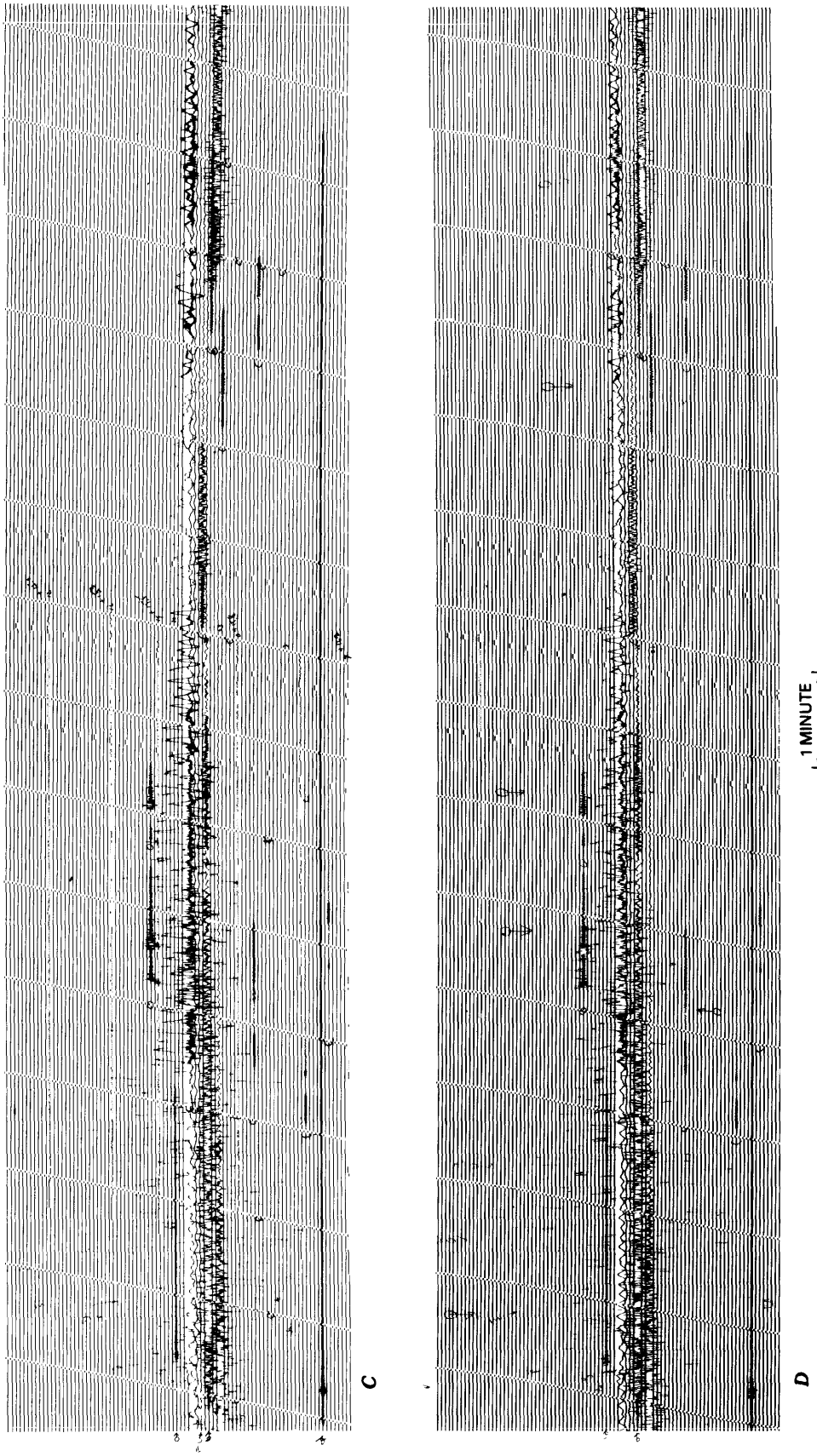

FIGURE 39.—Continued

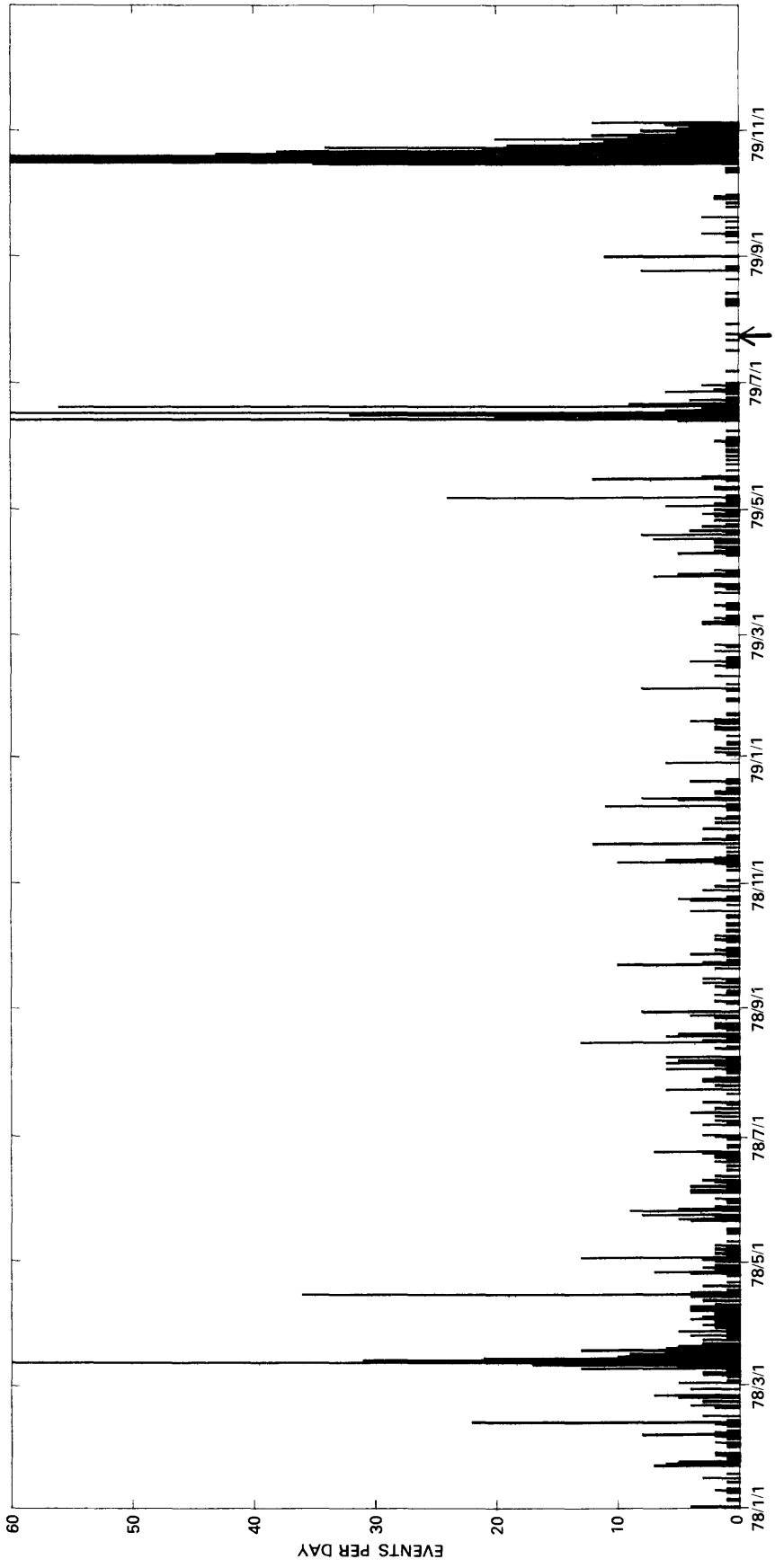

FIGURE 40.—Daily frequency of events detected by CEDAR system in area outlined in figure 37 from January 1, 1978, through November 5, 1979. Arrow marks change in instrumentation (see text).

above changes; these records are scanned independently of CEDAR system detection, and all events with coda lengths exceeding 25 s are timed and recorded. From this data set we compiled a list of all events with $S-P$ times at stations IKP and GLA of less than 12 s; the results agree with the existence of the period of low seismicity discussed above. At present, this quiet period appears to be real, although attempts to find an instrumental or procedural explanation will be continued.

If such a decrease in seismicity along the axis of the Imperial Valley did in fact occur, it would not be totally without precedent. Richter (1958) observed a decrease in swarm activity in the same area during the decade after the 1940 earthquake, and Johnson (1979) attributed this decrease to the dilatational quadrant of the 1940 earthquake, on the basis of a hydrologic model describing both episodic creep and swarm occurrence. Similarly, any dilatational component in the secular strain might be expected to decrease seismicity. For the interval 1973 through mid-1978 the geodetic results reported by Savage and others (1979) showed that dilatation in the northern Imperial Valley was negative (compression) and occurred at a constant rate. Beginning in late 1978 (Savage, 1979) this trend was reversed, 6 months before the sudden decrease in seismicity. Unfortunately, no data are available addressing the question whether an increase in extensional-strain rate may have accompanied the decrease in seismicity during mid-1979. Interestingly, it was during this period of apparent dilatation that the first normal events were observed on what has been suggested earlier as an extension of the San Andreas into the eastern Imperial Valley. Although these events are too small to provide focal mechanisms, first motions are generally compressive and agree with the normal mechanism (fig. 32) manifesting an east-west tension axis.

Figure 41 shows the spatial distribution of earthquakes during the quiet period. Seismicity seems to be more widely distributed than is generally apparent in a series of figures presented by Johnson (1979) covering comparable periods. A cluster of small earthquakes near the main-shock epicenter might be considered foreshocks, although they were uniformly distributed in time during this period and do not stand out as an obvious local increase in seismicity. Whether the records from these events are unusual in any respect is currently being studied.

The quiet period was immediately preceded by a swarm of earthquakes consisting of three discrete bursts of activity distributed over a 1-week interval during mid-June 1979. We do not know whether any special significance should be attributed to these events, although the epicentral distribution (fig. 42) lies just north of the area of most intense activity in the aftershock sequence near Brawley. This sequence also contrasts with previous swarms along the west margin of the Brawley seismic zone in being one of the most northerly during the preceding 6 years.

CONCLUSIONS

Aftershocks of the 1979 Imperial Valley earthquake were distributed in a complex pattern extending well beyond the zone of mapped surface rupture. The most intense activity was centered at the northwest end of surface faulting, and few aftershocks occurred near the main-shock epicenter. The largest aftershock ($M_L = 5.8$), which followed the main shock by nearly 8 hours, was apparently the result of sinistral motion on a conjugate northeast-trending fault north of Brawley, Calif. Thereafter, the aftershock clusters developed progressively over time along the Imperial fault trend at an apparent migration rate of approximately 2 km/d. A linear zone of events extending along the trend of the San Andreas fault south of the Salton Sea suggests sympathetic activation of a buried structure along the east margin of the Imperial Valley.

A remarkable 40-percent decrease in Imperial Valley seismicity that preceded the earthquake by 3½ months does not appear to be an artifact of either instrumentation or analysis. This decrease may in some way correlate with a change in east-west extension similar to that observed geodetically to the north during late 1978. Historical seismicity also suggests that an increase in the dilatational or possibly east-west extensional stress could have caused such a change in seismicity. Changes in the local secular-strain rate, which may ultimately have led to failure on the Imperial fault, may have preceded the main shock by several months and should have been observable had appropriate instrumentation been installed. Three small events clustered near the main-shock epicenter during the preceding months should be considered as candidate foreshocks, pending further investigation.

ACKNOWLEDGMENTS

We thank the CEDAR-system timers Anne Blanchard, Shirley Fisher, Peter German, Doug Given, Karen Richter, and Vic Lamanuzzi for their great diligence in the face of a seemingly endless task during the timing of initial aftershocks. Parts of the Imperial Valley base map were prepared by Peter T. German. This research was partly supported by U.S. Geological Survey Contract 14-08-0001-16719 and California Division of Mines and Geology Contract 5-0059.

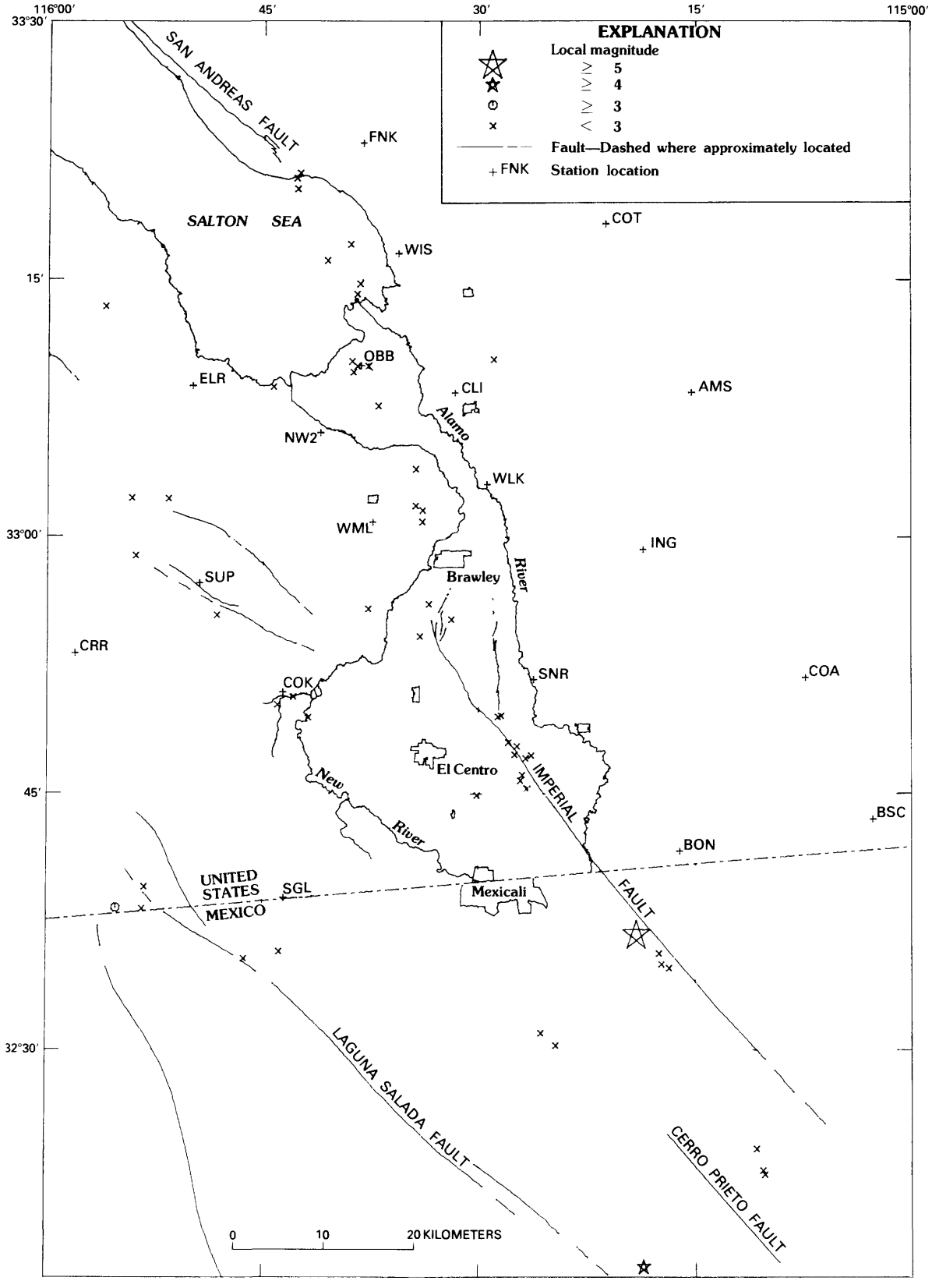

FIGURE 41.—Well-located earthquakes in Imperial Valley during 3½ months preceding October 15 main shock (large star), indicating quiet period in seismic activity.

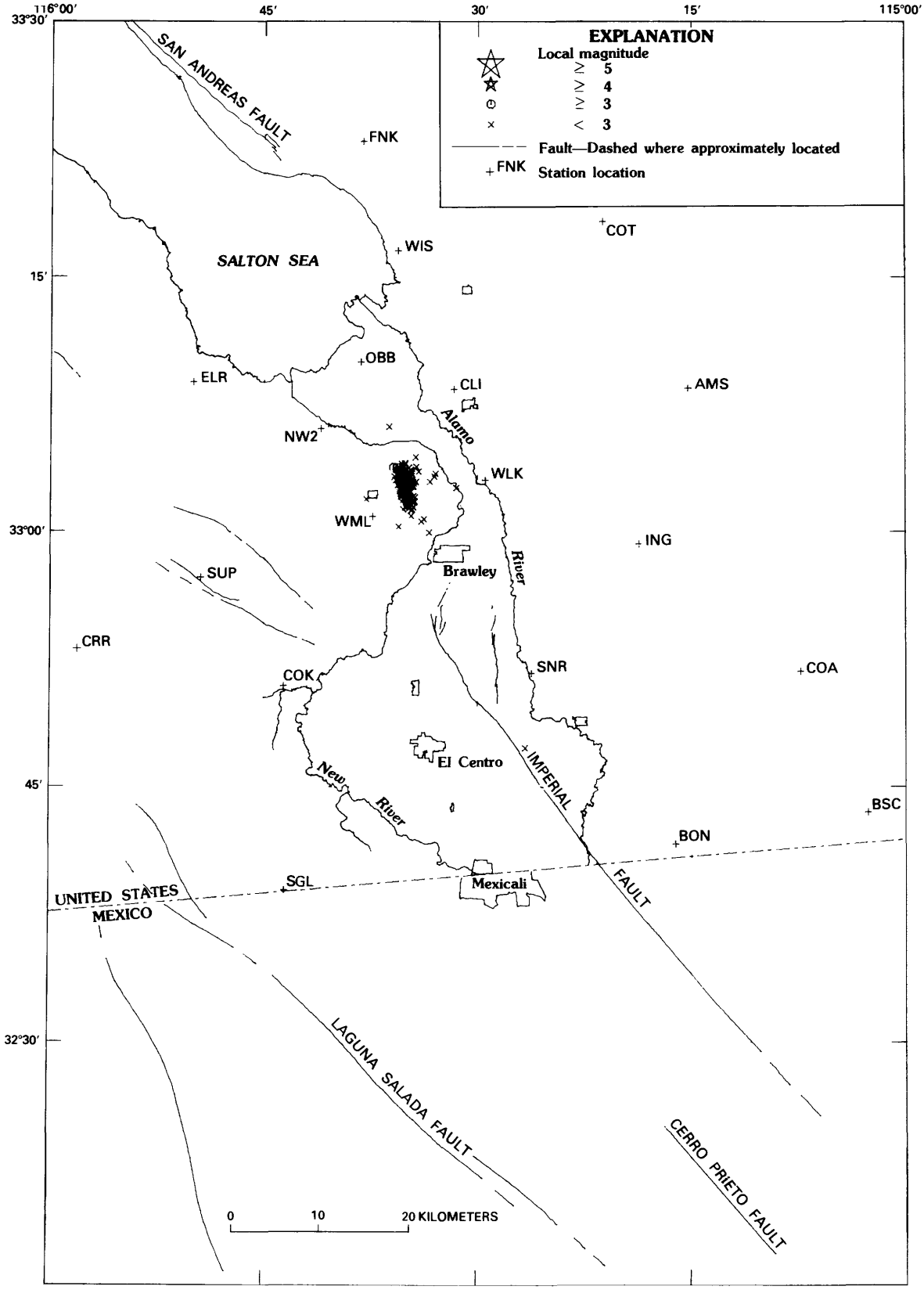

FIGURE 42.—Well-located earthquakes during an intense swarm near Brawley Calif., in mid-June 1979, immediately preceding quiet period shown in figure 41.

REFERENCES CITED

Goulty, N. R., Burford, R. O., Allen, C. R., Gilman, Ralph, Johnson, C. E., and Keller, R. P., 1978, Large creep events on the Imperial fault, California: Seismological Society of America Bulletin, v. 68, no. 2, p. 517–521.

Hill, D. P., 1977, A model for earthquake swarms: Journal of Geophysical Research, v. 82, no. 8, p. 1347–1352.

Johnson, C. E., 1979, CEDAR—an approach to the computer automation of short-period local seismic networks; seismotectonics of the Imperial Valley of southern California: Pasadena, California Institute of Technology, Ph. D. thesis, 343 p.

Johnson, C. E., and Hadley, D. M., 1976, Tectonic implications of the Brawley earthquakes swarm, Imperial Valley, California, January 1975: Seismological Society of America Bulletin, v. 66, no. 4, p. 1133–1144.

Keller, R. P., Allen, C. R., Gilman, Ralph, Goulty, N. R., and Hileman, J. A., 1978, Monitoring slip along major faults in southern California: Seismological Society of America Bulletin, v. 68, no. 4, p. 1187–1190.

Richter, C. F., 1958, Elementary seismology: San Francisco, W. H. Freeman, 768 p.

Savage, J. C., 1979, Crustal strain, *in* Seiders, W. H., compiler, Summaries of technical reports, volume 8: Menlo Park, Calif., U.S. Geological Survey, p. 317–319.

Savage, J. C., Prescott, W. H., Lisowski, M., and King, N., 1979, Deformation across the Salton Trough, California, 1973–1977: Journal of Geophysical Research, v. 84, no. B6, p. 3069–3079.

Trifunac, M. D., and Brune, J. N., 1970, Complexity of energy release during the Imperial Valley, California, earthquake of 1940: Seismological Society of America Bulletin, v. 60, no. 1, p. 137–160.

Whitcomb, J. H., 1973, A study of the velocity structure of the earth by the use of core phases (pt. 1); the 1971 San Fernando earthquake series focal mechanisms and tectonics (pt. 2): Pasadena, California Institute of Technology, Ph. D. thesis, 456 p.

Wiggins, R. A., 1972, The general linear inverse problem: Implication of surface waves and free oscillations for earth structure: Reviews of Geophysics and Space Physics, v. 10, no. 1, p. 251–285.

The Imperial Valley, California, Earthquake of October 15, 1979

GEOLOGICAL SURVEY PROFESSIONAL PAPER 1254

Contributions from:
American Iron and Steel Institute
California Department of Transportation
California Division of Mines and Geology
California Institute of Technology
Centro de Investigación Científica y Educación Superior de Ensenada, Baja California
H. J. Degenkolb & Associates, Consulting Structural Engineers
Imperial College, London
J. D. Raggett & Associates, Inc., Structural Engineers
Scripps Institution of Oceanography
U.S. Department of the Interior, Geological Survey
Universidad Nacional Autónoma de México

UNITED STATES GOVERNMENT PRINTING OFFICE, WASHINGTON: 1982